

## LETTERS

# Platensimycin is a selective FabF inhibitor with potent antibiotic properties

Jun Wang<sup>1\*</sup>, Stephen M. Soisson<sup>1\*</sup>, Katherine Young<sup>1</sup>, Wesley Shoop<sup>1†</sup>, Srinivas Kodali<sup>1</sup>, Andrew Galgoci<sup>1</sup>, Ronald Painter<sup>1</sup>, Gopalakrishnan Parthasarathy<sup>1</sup>, Yui S. Tang<sup>1</sup>, Richard Cummings<sup>1</sup>, Sookhee Ha<sup>1</sup>, Karen Dorso<sup>1</sup>, Mary Motyl<sup>1</sup>, Hiranthi Jayasuriya<sup>1</sup>, John Ondeyka<sup>1</sup>, Kithsiri Herath<sup>1</sup>, Chaowei Zhang<sup>1</sup>, Lorraine Hernandez<sup>1</sup>, John Allocco<sup>1</sup>, Ángela Basilio<sup>1</sup>, José R. Tormo<sup>1</sup>, Olga Genilloud<sup>1</sup>, Francisca Vicente<sup>1</sup>, Fernando Pelaez<sup>1</sup>, Lawrence Colwell<sup>1</sup>, Sang Ho Lee<sup>1</sup>, Bruce Michael<sup>1</sup>, Thomas Felcetto<sup>1</sup>, Charles Gill<sup>1</sup>, Lynn L. Silver<sup>1†</sup>, Jeffery D. Hermes<sup>1</sup>, Ken Bartizal<sup>1</sup>, John Barrett<sup>1‡</sup>, Dennis Schmatz<sup>1</sup>, Joseph W. Becker<sup>1</sup>, Doris Cully<sup>1</sup> & Sheo B. Singh<sup>1</sup>

Bacterial infection remains a serious threat to human lives because of emerging resistance to existing antibiotics. Although the scientific community has avidly pursued the discovery of new antibiotics that interact with new targets, these efforts have met with limited success since the early 1960s<sup>1,2</sup>. Here we report the discovery of platensimycin, a previously unknown class of antibiotics produced by *Streptomyces platensis*. Platensimycin demonstrates strong, broad-spectrum Gram-positive antibacterial activity by selectively inhibiting cellular lipid biosynthesis. We show that this anti-bacterial effect is exerted through the selective targeting of  $\beta$ -ketoacyl-(acyl-carrier-protein (ACP)) synthase I/II (FabF/B) in the synthetic pathway of fatty acids. Direct binding assays show that platensimycin interacts specifically with the acyl-enzyme intermediate of the target protein, and X-ray crystallographic studies reveal that a specific conformational change that occurs on acylation must take place before the inhibitor can bind. Treatment with platensimycin eradicates *Staphylococcus aureus* infection in mice. Because of its unique mode of action, platensimycin shows no cross-resistance to other key antibiotic-resistant strains tested, including methicillin-resistant *S. aureus*, vancomycin-intermediate *S. aureus* and vancomycin-resistant enterococci. Platensimycin is the most potent inhibitor reported for the FabF/B condensing enzymes, and is the only inhibitor of these targets that shows broad-spectrum activity, *in vivo* efficacy and no observed toxicity.

Bacterial type II fatty-acid synthesis (FASII) is an attractive target for antibacterial drug discovery<sup>3–7</sup>. The initiation condensing enzyme, FabH, and elongation condensing enzymes, FabF/B, are essential components of fatty-acid biosynthesis<sup>8–11</sup> and are highly conserved among key pathogens. Although no drugs targeting condensing enzymes are used clinically, cerulenin<sup>12</sup> and thiolactomycin<sup>13</sup> selectively inhibit the condensation enzymes FabF/B and FabH.

Systematic screening of 250,000 natural product extracts (83,000 strains in three growth conditions), with the use of a combination of target-based whole-cell and biochemical assays, led to the identification of a potent and selective small molecule from a strain of *Streptomyces platensis* recovered from a soil sample collected in South Africa. This molecule, platensimycin ( $C_{24}H_{27}NO_7$ , relative molecular mass 441.47), comprises two distinct structural elements connected by an amide bond (Fig. 1a).

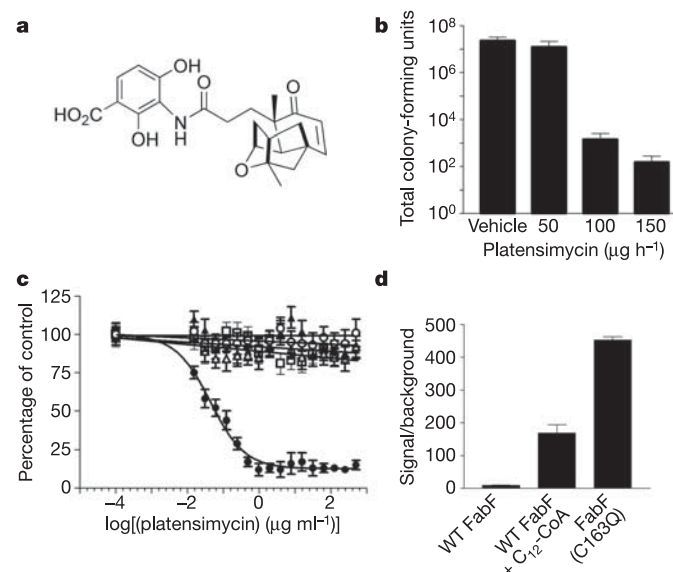


**Figure 1 | Characterization of platensimycin.** **a**, Structure of platensimycin. **b**, *In vivo* studies on platensimycin. Dosing at  $50\text{ }\mu\text{g h}^{-1}$  showed small decrease in viable *S. aureus* cells from the infected kidney. However, a  $10^4$ – $10^5$  fold decrease (4 and 5 log reduction) were achieved with 100 and  $150\text{ }\mu\text{g h}^{-1}$ , respectively. Dosing at  $150\text{ }\mu\text{g h}^{-1}$  showed 40% of the kidneys with no viable *S. aureus*, whereas dosing at  $100\text{ }\mu\text{g h}^{-1}$  showed 20% of the kidneys without detectable viable *S. aureus*. Error bars indicate s.d. observed with five infected mice. The results were confirmed by a repeat experiment. **c**, Whole-cell labelling assay<sup>16</sup> with platensimycin. The assay was performed with a serial dilution of platensimycin, starting at  $500\text{ }\mu\text{g ml}^{-1}$ . Platensimycin showed no significant inhibition against syntheses of DNA (open circles), cell wall (filled triangles), protein (open squares) and RNA (open triangles) but greatly inhibited phospholipid synthesis (filled circles), providing an  $IC_{50}$  value of  $0.1\text{ }\mu\text{g ml}^{-1}$ . Error bars indicate s.d. for three individual experiments. **d**, Direct binding assay results of [ $^3\text{H}$ ]dihydroplatensimycin and *E. coli* FabF (ecFabF) in the presence and absence of n-dodecanoyl coenzyme A (lauroyl-CoA;  $C_{12}$ -CoA) and the  $C_{16}3Q$  mutant protein. Error bars indicate s.d. observed with six replicate wells. Experimental details are given in Supplementary Information.

<sup>1</sup>Merck Research Laboratories, Rahway, New Jersey 07065, USA. <sup>†</sup>Present addresses: DuPont Stine-Haskell Research Center, 1090 Elkton Road, Newark, Delaware 19711, USA (W.S.); LL Silver Consulting, 3403 Park Place, Springfield, New Jersey 07081, USA (L.L.S.).

<sup>\*</sup>These authors contributed equally to the work.

<sup>‡</sup>Deceased.

Platensimycin shows potent, broad-spectrum Gram-positive activity *in vitro* (Table 1; methods described in ref. 14) and exhibits no cross-resistance to other key antibiotic-resistant bacteria including methicillin-resistant *S. aureus*, vancomycin-intermediate *S. aureus*, vancomycin-resistant enterococci, and linezolid-resistant and macrolide-resistant pathogens. Platensimycin showed antibacterial activity against efflux-negative *Escherichia coli* (*tolC*), but not against wild-type *E. coli*, indicating that efflux mechanisms, and not compound specificity, limit the effectiveness of platensimycin in *E. coli* and possibly other Gram-negative bacteria. Low mammalian cell toxicity (50% inhibitory concentration ( $IC_{50}$ )  $> 1,000 \mu\text{g ml}^{-1}$  in a HeLa cytotoxicity assay) and lack of antifungal activity (more than  $64 \mu\text{g ml}^{-1}$ ) further suggests that platensimycin acts selectively. Platensimycin exhibited minimum inhibitory concentration (MIC) values of 0.5 and  $1 \mu\text{g ml}^{-1}$  against *S. aureus* and *S. pneumoniae*, respectively.

The efficacy of platensimycin *in vivo* was evaluated in a mouse model of a disseminated *S. aureus* infection. In this experiment, mice were cannulated in the jugular vein and drug was delivered with a continuous-delivery pump. The compound showed excellent efficacy with a  $10^4$ – $10^5$  fold decrease (4–5 log reduction) of *S. aureus* infection over a 24-h treatment period (Fig. 1b) at 100 and  $150 \mu\text{g h}^{-1}$  with no indication of toxicity. Monitoring of plasma concentration during treatment provided a dose-dependent exposure level of about  $0.17 \mu\text{g ml}^{-1}$  (compound administered at  $25 \mu\text{g h}^{-1}$ ),  $0.32 \mu\text{g ml}^{-1}$  ( $50 \mu\text{g h}^{-1}$ ) and about  $0.6 \mu\text{g ml}^{-1}$  ( $100 \mu\text{g h}^{-1}$ ). The efficacious dose of  $100 \mu\text{g h}^{-1}$  produced a plasma exposure level of  $0.6 \mu\text{g ml}^{-1}$ , which is lower than the MIC *in vitro* ( $2 \mu\text{g ml}^{-1}$ ) determined in the presence of serum (Table 1, MIC tested *in vitro* with serum to mimic the animal test conditions), indicating a possible minimal serum effect *in vivo*. No toxicity was observed in similar experiments in which mice received 300 or  $250 \mu\text{g h}^{-1}$  for 24 h, and in a longer study in which  $50 \mu\text{g h}^{-1}$  was administered for 9 days followed by  $100 \mu\text{g h}^{-1}$  for 8 days.

In whole-cell labelling experiments (Fig. 1c), platensimycin showed selective inhibition of lipid biosynthesis in *S. aureus* with an  $IC_{50}$  of  $0.1 \mu\text{g ml}^{-1}$ . Platensimycin did not inhibit DNA, RNA, protein or cell wall biosynthesis at concentrations up to  $500 \mu\text{g ml}^{-1}$ , thereby confirming its selectivity. Similar results were obtained with *S. pneumoniae*, in which the  $IC_{50}$  for inhibition of cellular lipid biosynthesis was  $0.8 \mu\text{g ml}^{-1}$ . The correspondence between MICs and  $IC_{50}$  values for the inhibition of cellular lipid biosynthesis (Table 1) strongly indicates that the antibiotic kills bacteria entirely through the inhibition of fatty-acid biosynthesis.

**Table 1 | Microbiological profiles and toxicity of platensimycin and linezolid**

Organism and genotype	Platensimycin	Linezolid
Antibacterial activity (MIC, $\mu\text{g ml}^{-1}$ )*		
<i>S. aureus</i> (MSSA)	0.5	4
<i>S. aureus</i> + serum	2	4
<i>S. aureus</i> (MRSA)	0.5	2
<i>S. aureus</i> (MRSA, macrolide <sup>R</sup> )	0.5	2
<i>S. aureus</i> (MRSA, linezolid <sup>R</sup> )	1	32
<i>S. aureus</i> (VISA, vancomycin <sup>I</sup> )	0.5	2
<i>Enterococcus faecalis</i> (macrolide <sup>R</sup> )	1	1
<i>Enterococcus faecium</i> (VRE)	0.1	2
<i>S. pneumoniae</i> <sup>I</sup>	1	1
<i>E. coli</i> (wild-type)	$>64$	$>64$
<i>E. coli</i> ( <i>tolC</i> )	16	32
Toxicity ( $\mu\text{g ml}^{-1}$ )		
HeLa MTT ( $IC_{50}$ )	$>1,000$	$>100$
<i>Candida albicans</i> (MIC)	$>64$	$>64$

\*A concentration of  $1 \mu\text{g ml}^{-1}$  equals  $2.27 \mu\text{M}$  for platensimycin and  $2.96 \mu\text{M}$  for linezolid.

<sup>I</sup>Cells were inoculated at  $10^5$  colony-forming units followed by incubation overnight at  $37^\circ\text{C}$  with a serial dilution of compounds in Todd–Hewitt broth.

Linezolid is a synthetically derived agent that has been in clinical use since 2000. MRSA, methicillin-resistant *S. aureus*; MSSA, methicillin-susceptible *S. aureus*; MTT, 3-(4,5-dimethylthiazol-2-yl)-2,5-diphenyl-2H-tetrazolium bromide; VISA, vancomycin-intermediate *S. aureus*; VRE, vancomycin-resistant *Enterococcus*.

The target selectivity of platensimycin was first determined with *S. aureus* strains either expressing antisense *FabF* RNA (AS-*fabF*) or overexpressing *FabF* protein. Antisense expression decreases expression of the targeted protein, making the cells more sensitive to exogenous inhibitors of the targeted protein. Hence, antisense plates show larger inhibition zones than wild-type control plates<sup>15</sup> (Supplementary Fig. S1a), whereas overexpression strains show the opposite effect (Supplementary Fig. S1b). In comparison with cerulenin, platensimycin showed a 200-fold greater potency and similar *FabF* target selectivity in both assays, indicating that *FabF* is the sole target of platensimycin for the inhibition of bacterial growth. This mechanism of action was further confirmed with a cell-free gel-elongation assay<sup>16</sup> (Supplementary Fig. S2a). Potency analysis of platensimycin against FASII *S. aureus* enzymes in the gel-elongation assay provided an  $IC_{50}$  of  $0.2 \mu\text{g ml}^{-1}$  (Supplementary Fig. S2b). This value is consistent with the  $IC_{50}$  ( $0.1 \mu\text{g ml}^{-1}$ ) obtained in the whole-cell labelling assay, indicating that platensimycin has good permeability through the cell membrane.

Single-enzyme catalytic assays showed that platensimycin is a potent inhibitor of *FabF* with an  $IC_{50}$  of  $48$  and  $160 \text{ nM}$  for *S. aureus* and *E. coli* enzymes, respectively (Supplementary Fig. S3a). In a similar catalytic assay, platensimycin showed weak inhibition of *S. aureus* *FabH*, with an  $IC_{50}$  of  $67 \mu\text{M}$  (Supplementary Fig. S3b).

To demonstrate that platensimycin inhibits *FabF* by targeting the protein directly, we developed a direct binding assay employing a radioactive derivative of platensimycin ( $^3\text{H}$ -dihydroplatensimycin; Supplementary Fig. S4a) and the purified, recombinant enzyme. Initial assays yielded binding affinities significantly less than those expected from the potency observed in other *in vitro* and *in vivo*

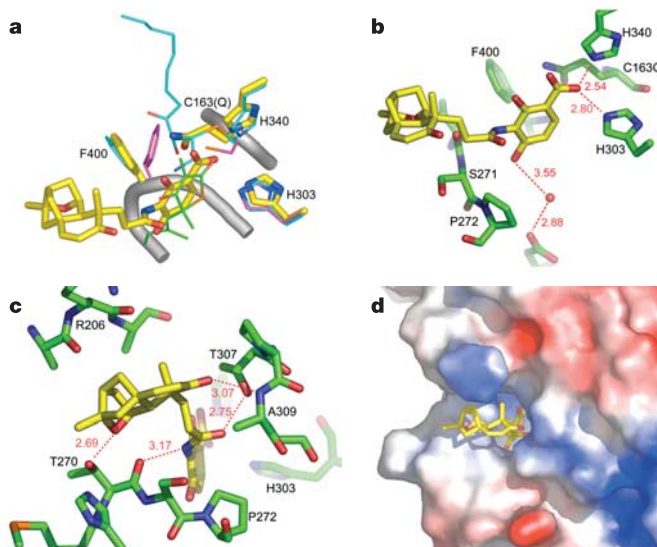


**Figure 2 | Interactions of platensimycin with ecFabF(C163Q) and comparison with the apo structure.** **a**, Superposition of platensimycin (yellow, thicker sticks) on ecFabF, with thiolactomycin (green) and cerulenin (cyan) shown for reference. Side chains discussed in the text are labelled and coloured as described above. **b**, Interactions between the benzoic acid ring of platensimycin (yellow) and ecFabF(C163Q). Side chains from the protein discussed in the text are labelled and coloured green. **c**, Interactions of ecFabF with the amide linker and ketolide of platensimycin. The colour scheme is the same as in **b**. **d**, The solvent-accessible surface area of FabF, coloured according to electrostatic potential. Platensimycin is depicted as a stick figure and coloured yellow, and is shown to be partly exposed to solvent. Platensimycin buries  $345 \text{ \AA}^2$  of solvent-accessible surface area on ecFabF, as calculated with areaimol<sup>24,25</sup>. Of that surface area,  $122 \text{ \AA}^2$  is a direct result of the ketolide portion of the molecule, highlighting its important contribution to platensimycin binding. Significant interatomic distances (in Å) are marked in **b** and **c** with red dashed lines and numbers.

assays. Changes in experimental conditions (for example pH or ionic strength) did not strongly increase inhibitor binding. Because the condensing enzymes catalyse a complex series of reactions using multiple substrates in a ping-pong mechanism<sup>17</sup>, we hypothesized that platensimycin might act by inhibiting a major species of the catalytic cycle, the covalent acyl-enzyme intermediate. We prepared a surrogate intermediate by adding lauroyl-CoA to mimic the natural acyl-ACP substrate, which results in the formation of a transiently stable covalent acyl-enzyme complex through the formation of a thioester with the cysteine (Cys 163) at the active site. Addition of this substrate increased the binding signal 19-fold relative to that obtained with the apoenzyme (Fig. 1d). This finding is consistent with the hypothesis that formation of the acyl-enzyme intermediate is essential for platensimycin binding. Titration studies of various inhibitors performed in the presence of lauroyl-CoA indicate a binding  $IC_{50}$  of 19 nM for platensimycin, 97 nM for dihydroplatensimycin and 1.1  $\mu$ M for thiolactomycin (Supplementary Fig. S5).

Attempts to obtain homogeneous preparations of acylated, wild-type FabF enzyme suitable for crystallographic studies were not successful, presumably as a result of the short half-life of the thioester intermediate. For this reason, various mutant proteins were generated in attempts to stabilize the acyl-enzyme intermediate. On the basis of previous literature reports, we mutated Cys 163 to serine in an effort to stabilize the acyl-enzyme intermediate<sup>18</sup>; however, the occupancies of the acyl chain and platensimycin in the crystals were too low to yield a high-quality structure. A similar mutation (K335A)<sup>19</sup> also did not show any inhibitor binding because of unexpected, mutation-induced, conformational changes (Supplementary Information). Mutation of the active-site cysteine in an animal  $\beta$ -ketoacyl synthase domain to glutamine (C161Q) results in an enzyme with potent malonyl decarboxylase activities<sup>20</sup>, possibly by sterically mimicking the formation of the acyl-enzyme intermediate. We generated the corresponding *E. coli* (ec)FabF(C163Q) mutant and found that this mutant enzyme shows a 50-fold increase in apparent binding of platensimycin compared with wild-type enzyme (Fig. 1d). The 2.6-fold increase over the signal observed with wild-type enzyme and lauroyl-CoA is probably due to the partial acylation of FabF with this non-natural substrate, whereas the C163Q mutation presumably pre-positions nearly all components of the FabF catalytic machinery in the acyl-enzyme conformation, resulting in more robust binding. This interpretation is supported by structural studies of the unliganded ecFabF(C163Q) protein (Supplementary Information), showing that this mutation results in a protein with all the characteristic features of the acyl-enzyme structure. In particular, the mutation induces a change in the side chain of Phe 400, converting it from a 'closed' conformation—one that blocks platensimycin binding in the wild-type apoenzyme—to an 'open' conformation in the mutant (see below; Fig. 2a, and Supplementary Fig. S6).

The 2.6- $\text{\AA}$  structure of ecFabF(C163Q) in complex with platensimycin shows that the antibiotic binds in the malonyl subsite of FabF (Fig. 2a), with its benzoic acid ring in roughly the same orientation as thiolactomycin<sup>21</sup>, where it is positioned to interact with important residues of the catalytic machinery<sup>19</sup> (Fig. 2b). The carboxylate of the benzoic acid ring engages the active-site histidine residues (His 303 and His 340) that are part of the conserved His-His-Cys catalytic triad (Fig. 2b). The distances between the carboxylate and His 303 (2.5  $\text{\AA}$ ) and His 340 (2.8  $\text{\AA}$ ), together with previous reports that these histidines are involved in the decarboxylation reaction<sup>19</sup> and may be protonated to stabilize negative charges during the catalytic cycle<sup>22</sup>, are all indicative of a strong interaction with a probable ionic component. The location and proximity of the carboxylate in platensimycin to the catalytic histidines further suggests that this interaction mimics the interaction between the natural substrate, malonate, and the enzyme.

The benzoic acid ring stacks edge-to-face against the open conformation of Phe 400 (for discussions see Supplementary Information),

the gatekeeper residue that separates the malonyl-binding and acyl-binding subsites. The hydroxyl group *para* to the acid makes weak water-mediated hydrogen bonds to protein residues in the extreme reaches of the malonyl subsite (Fig. 2b). The observation of the energetically favourable edge-to-face interaction<sup>23</sup> between the benzoic acid ring and Phe 400 reveals why platensimycin binds selectively to the acyl-enzyme intermediate: In the apoenzyme the closed conformation of Phe 400 would clash sterically with platensimycin's benzoic acid ring and could not make as favourable a stacking interaction with the inhibitor (Fig. 2a, b).

The amide-linked, pentacyclic, ketolide portion of platensimycin is positioned in the mouth of the active site and is partly exposed to solvent (Fig. 2c, d). The amide linker between the benzoic acid ring and the ketolide makes two critical hydrogen bonds to the protein. The carbonyl oxygen bonds to the side chain of Thr 307, and the amide nitrogen interacts with the backbone carbonyl of Thr 270. The ketolide itself makes numerous van der Waals interactions with the protein and exploits two direct hydrogen bonds that contribute to binding specificity. The enone carbonyl oxygen makes a hydrogen bond to the backbone amide of Ala 309, and the ether oxygen makes a hydrogen bond to the side-chain hydroxyl of Thr 270. The structural results described here are fully consistent with a model for FabF inhibition by platensimycin based on competition with malonyl-ACP for the malonyl subsite of the enzyme. The nature of the interactions between platensimycin and FabF indicates that resistance arising through the mutation of target protein is unlikely (Supplementary Information).

The novel chemical architecture and unique mode of action and the encouraging results *in vivo*, coupled with the biochemical and structural studies, emphasize that platensimycin provides a great opportunity for the development of critically needed antibiotics.

## METHODS

**Screening for natural product inhibitors.** Fermentation broth derived from *Streptomyces platensis* grown in a liquid medium was extracted with an equal volume of acetone and filtered. Acetone was removed by blowing with nitrogen and the aqueous portion was tested on to FabF (target-based) two-plate assay<sup>15</sup> followed by confirmation in a FASII assay<sup>16</sup>.

**Isolation of platensimycin.** The active acetone extract was charged on a reverse-phase Amberchrome resin and eluted with a linear gradient of aqueous methanol. Each fraction was tested in the FabF two-plate assay, and fractions that showed activity (larger zone on the antisense plate than on the control plate) were pooled and rechromatographed on a Sephadex LH 20 column in methanol. The resulting fractions with FabF activity were purified by reverse-phase C<sub>8</sub> high-performance liquid chromatography with a linear gradient of aqueous acetonitrile (containing trifluoroacetic acid), yielding platensimycin (2 mg, titre 3 mg l<sup>-1</sup>) as an amorphous powder. The structure was elucidated by two-dimensional NMR analysis and mass spectra, and confirmed by single-crystal X-ray analysis.

**In vivo study.** Mice were challenged intraperitoneally with *S. aureus*. Platensimycin was infused continuously intravenously at 100  $\mu$ l h<sup>-1</sup> for 24 h. After treatment, mice were killed and kidneys removed for the evaluation of bacterial infection (see Supplementary Information for further details).

**Whole-cell labelling.** The whole-cell labelling assay has been described previously<sup>16</sup>.

**FabF direct binding assay.** The binding of His-tagged recombinant FabF and [<sup>3</sup>H]dihydroplatensimycin was measured in a scintillation proximity assay format. Details are described in Supplementary Information.

**Crystallographic study.** X-ray data collection and determination of structures are detailed in Supplementary Information.

Received 10 March; accepted 6 April 2006.

1. Singh, S. B. & Barrett, J. F. Empirical antibacterial drug discovery—foundation in natural products. *Biochem. Pharmacol.* 71, 1006–1015 (2006).
2. Butler, M. S. & Buss, A. D. Natural products—the future scaffolds for novel antibiotics? *Biochem. Pharmacol.* 71, 919–929 (2006).
3. Campbell, J. W. & Cronan, J. E. Bacterial fatty acid biosynthesis: Targets for antibacterial drug discovery. *Annu. Rev. Microbiol.* 55, 305–332 (2001).
4. Zhang, Y.-M., Marrakchi, H., White, S. W. & Rock, C. O. The application of computational methods to explore the diversity and structure of bacterial fatty acid synthase. *J. Lipid Res.* 44, 1–10 (2003).

5. Heath, R. J. & Rock, C. O. Fatty acid biosynthesis as a target for novel antibiotics. *Curr. Opin. Investig. Drugs* **5**, 146–153 (2004).
6. Smith, S., Witkowski, A. & Joshi, A. K. Structural and functional organization of the animal fatty acid synthase. *Prog. Lipid Res.* **42**, 289–317 (2003).
7. White, S. W., Zheng, J., Zhang, Y. M. & Rock, C. O. The structural biology of type II fatty acid biosynthesis. *Annu. Rev. Biochem.* **74**, 791–831 (2005).
8. Revill, W. P., Bibb, M. J., Scheu, A. K., Kieser, H. J. & Hopwood, D. A. Beta-ketoacyl acyl carrier protein synthase III (FabH) is essential for fatty acid biosynthesis in *Streptomyces coelicolor* A3(2). *J. Bacteriol.* **183**, 3526–3530 (2001).
9. Lai, C.-Y. & Cronan, J. E.  $\beta$ -Ketoacyl-acyl carrier protein synthase III (FabH) is essential for bacterial fatty acid synthesis. *J. Biol. Chem.* **278**, 51494–51503 (2003).
10. Tsay, J., Rock, C. & Jackowski, S. Overproduction of beta-ketoacyl-acyl carrier protein synthase I imparts thiolactomycin resistance to *Escherichia coli* K-12. *J. Bacteriol.* **174**, 508–513 (1992).
11. Schujman, G. E., Choi, K. H., Altabe, S., Rock, C. O. & de Mendoza, D. Response of *Bacillus subtilis* to cerulenin and acquisition of resistance. *J. Bacteriol.* **183**, 3032–3040 (2001).
12. Matsumae, A., Nomura, S. & Hata, T. Studies on cerulenin. IV. Biological characteristics of cerulenin. *J. Antibiot. (Tokyo)* **17**, 1–7 (1964).
13. Noto, T., Miyakawa, S., Oishi, H., Endo, H. & Okazaki, H. Thiolactomycin, a new antibiotic. III. *In vitro* antibacterial activity. *J. Antibiot. (Tokyo)* **35**, 401–410 (1982).
14. Wang, J. *et al.* Discovery of a small molecule that inhibits cell division by blocking Ftsz, a novel therapeutic target of antibiotics. *J. Biol. Chem.* **278**, 44424–44428 (2003).
15. Young, K. *et al.* Discovery of FabH/FabF inhibitors from natural products. *Antimicrob. Agents Chemother.* **50**, 519–526 (2006).
16. Kodali, S. *et al.* Determination of selectivity and efficacy of fatty acid synthesis inhibitors. *J. Biol. Chem.* **280**, 1669–1677 (2005).
17. Heath, R. J. & Rock, C. O. The Claisen condensation in biology. *Nat. Prod. Rep.* **19**, 581–596 (2002).
18. Olsen, J. G., Kadziola, A., von Wettstein-Knowles, P., Siggaard-Andersen, M. & Larsen, S. Structures of beta-ketoacyl-acyl carrier protein synthase I complexed with fatty acids elucidate its catalytic machinery. *Structure (Camb)* **9**, 233–243 (2001).
19. McGuire, K. A., Siggaard-Andersen, M., Bangera, M. G., Olsen, J. G. & von Wettstein-Knowles, P.  $\beta$ -Ketoacyl-[acyl carrier protein] synthase I of *Escherichia coli*: aspects of the condensation mechanism revealed by analyses of mutations in the active site pocket. *Biochemistry* **40**, 9836–9845 (2001).
20. Witkowski, A., Joshi, A. K., Lindqvist, Y. & Smith, S. Conversion of a beta-ketoacyl synthase to a malonyl decarboxylase by replacement of the active-site cysteine with glutamine. *Biochemistry* **38**, 11643–11650 (1999).
21. Price, A. C. *et al.* Inhibition of beta-ketoacyl-acyl carrier protein synthases by thiolactomycin and cerulenin. Structure and mechanism. *J. Biol. Chem.* **276**, 6551–6559 (2001).
22. Huang, W. *et al.* Crystal structure of beta-ketoacyl-acyl carrier protein synthase II from *E. coli* reveals the molecular architecture of condensing enzymes. *EMBO J.* **17**, 1183–1191 (1998).
23. Hunter, C. A., Singh, J. & Thornton, J. M. Pi–pi interactions: the geometry and energetics of phenylalanine–phenylalanine interactions in proteins. *J. Mol. Biol.* **218**, 837–846 (1991).
24. Lee, B. & Richards, F. M. The interpretation of protein structures: estimation of static accessibility. *J. Mol. Biol.* **55**, 379–400 (1971).
25. Collaborative Computational Project No. 4, The CCP4 Suite: Programs for protein crystallography. *Acta Crystallogr. D Biol. Crystallogr.* **50**, 760–763 (1994).

**Supplementary Information** is linked to the online version of the paper at [www.nature.com/nature](http://www.nature.com/nature).

**Acknowledgements** Use of the IMCA-CAT beamline 17-ID (or 17-BM) at the Advanced Photon Source was supported by the companies of the Industrial Macromolecular Crystallography Association through a contract with the Center for Advanced Radiation Sources at the University of Chicago. We thank the staff of IMCA-CAT for their able assistance in data collection. This paper is dedicated to the late John Barrett for his strong contributions to antibiotic research.

**Author Contributions** J.W. and S.B.S. led the discovery, microbiological, biochemical characterization and natural products chemistry. S.M.S. coordinated X-ray crystallographic analysis and direct binding assay development.

**Author Information** Reprints and permissions information is available at [npg.nature.com/reprintsandpermissions](http://npg.nature.com/reprintsandpermissions). Coordinates and structure factors for all structures presented in this paper have been deposited with the PDB under accession numbers 2GFV, 2GFW, 2GFX, and 2GFY. The authors declare no competing financial interests. Correspondence and requests for materials should be addressed to J.W. (jun\_wang2@merck.com), S.M.S. (stephen\_soisson@merck.com) or S.B.S. (sheo\_singh@merck.com).